$L_{2,3}$-subshell x-ray fluorescence and Coster-Kronig yields at $Z=64$ and 67

B. E. Gnade, R. A. Braga, and R. W. Fink
School of Chemistry, Georgia Institute of Technology, Atlanta, Georgia 30332
(Received 10 October 1979)

The total Coster-Kronig transition probability f_{23} for the L_2-L_3 transition and the L_2 and L_3 subshell x-ray fluorescence yields ω_2 and ω_3 were measured utilizing resolved L-K x-ray coincidence techniques for $Z=64$ and 67 with radioactive sources of 4.68 yr ^{155}Eu and 10.4 h ^{165}Er, respectively. Improved accuracy in the results is achieved by advances in the experimental method. The values of f_{23} are 0.130 ± 0.012 and 0.115 ± 0.011 at $Z=64$ and 67, respectively, and of ω_2 and ω_3 are 0.165 ± 0.022 and 0.161 ± 0.019 at $Z=64$, and 0.186 ± 0.023 and 0.180 ± 0.020 at $Z=67$, respectively. The quoted uncertainties are twice the average deviation from the mean of 12 values of f_{23} and two values each of ω_2 and ω_3, and arise predominantly from systematic errors.

[RADIOACTIVITY ^{155}Eu; ^{165}Er; measured ω_2, ω_3, f_{23} in $L_{2,3}$ subshells; $XX\cdot t$ coin; Ge(HP)-Si(Li) detectors.]

I. INTRODUCTION

This investigation of the $L_{2,3}$ subshell x-ray fluorescence yields and Coster-Kronig total transition probability at $Z=64$ and 67 was carried out to provide a test of theory and improved values for experimental applications. Recently, some new relativistic calculations of radiationless transition rates to L-subshell vacancy states have been performed[1] for selected elements with $Z=70$ to 96. In this region, these calculated relativistic L-subshell widths agree with experimental values better than previous nonrelativistic calculations.[2-4] Relativistic calculations for lower-Z elements, however, are not yet available, but they are of interest in the light of the new experimental results reported here and our current effort to extend the measurements to $Z=54$.

Accurate experimental values of L-subshell fluorescence and Coster-Kronig yields also are important in many practical applications, ranging from elemental analysis by x-ray emission techniques to basic studies of nuclear and atomic processes leading to emission of x rays and Auger electrons, such as electron capture, internal conversion, and ionization cross section measurements.

Previous measurements of the total L_2-L_3 Coster-Kronig transition probability f_{23} at $Z=65$ (Ref. 5) and (Refs. 6 and 7) resulted in higher values than those found in the present work, whereas the discrepancies between previous and present values of the L-subshell x-ray fluorescence yields ω_2 and ω_3 are small. The present work is based on significant improvements in the experimental technique and in data evaluation. These advances include (1) an improved electronics system and the use of much faster coincidence timing (made possible by using a three-parameter multichannel $XX\cdot t$ coincidence configuration); (2) much better resolution and spectral quality of the K x rays through the use of a new, state-of-the-art ion-implanted Ge(HP) detector; (3) collimation to drastically reduce Compton backscattering from one detector to the other in the 180° coincidence geometry used; and (4) application of a new method[8] for the direct experimental determination of the absolute correction for tailing of $K\alpha_1$ events into the $K\alpha_2$ x-ray peak.

II. BASIS OF THE EXPERIMENTAL METHOD

The basic physical relationships among the L subshells involved in the determination of ω_2, ω_3, and f_{23} can be found in the 1972 review by Bambynek *et al.*,[9] but the working equations containing the detailed experimental corrections are not included. They appear in various forms scattered throughout the literature with occasional unfortunate errors. For this reason, we consolidate and present here in a standardized form all of the necessary working experimental equations for the determination of ω_2, ω_3, and f_{23}. Where applicable, the notation follows that of Rao *et al.*[10]

The present experiment measures the quantities ω_3, f_{23}, and ν_2, the latter representing the total number of L-shell x rays (from all shells and not just from the radiative filling of an L_2-subshell vacancy) that result per primary vacancy in the L_2 subshell.[9,10] Measurement of ν_2, f_{23}, and ω_3 proceeds directly from the relationships

$$\nu_2=\frac{C_{L(K\alpha_2)}}{I_{K\alpha_2}\epsilon_L\epsilon_c}\ , \tag{1}$$

$$f_{23}=\frac{C_{L_3X(K\alpha_2)}C_{(K\alpha_1)}}{C_{L_3X(K\alpha_1)}(\theta)C_{(K\alpha_2)}}\,, \tag{2}$$

$$\omega_3=\frac{C_{L(K\alpha_1)}(\theta)}{I_{K\alpha_1}\epsilon_L\epsilon_c}\,, \tag{3}$$

from which the value of ω_2 is obtained through the relationship

$$\omega_2=\nu_2-f_{23}\omega_3\,. \tag{4}$$

In Eqs. (1)–(4), $C_{L(K\alpha_2)}$ is the total number of L x-ray counts gated by $K\alpha_2$ x rays (after correction for continuum, nuclear cascading if present, chance coincidences, and for L x-ray coincidences arising from $K\alpha_1$ tailing events falling within the $K\alpha_2$ gate $G2$). Coincidence gates $G1$ through $G5$ and $G(K_\beta)$ are shown in Fig. 1. $I_{K\alpha_2}$ is the intensity (counts) of $K\alpha_2$ *singles* events falling within the energy region defined by $G2$ (corrected for background and *singles* $K\alpha_1$ tail events). (Note that $I_{K\alpha_1}$ and $I_{K\alpha_2}$ are the intensities of $K\alpha_1$ and $K\alpha_2$ *singles* events falling within the energy region of the *singles* spectrum defined by $G1$ and $G2$, respectively, Fig. 1, and are *not* coincidence intensities.) ϵ_L is the overall L x-ray detection efficiency averaged over the L x-ray energy region of interest and incorporates geometry and air-window attenuation, etc., and ϵ_c is the coincidence efficiency determined experimentally. $C_{L_3X(K\alpha_2)}$ represents the total number of L x-ray coincidence counts gated by $K\alpha_2$ x rays (corrected for background, nuclear cascading if present, chance coincidences, and for $K\alpha_1$ coincidence tail events in gate $G2$). The quantity $C_{L_3X(K\alpha_2)}$ arises from L_3-X shell transitions, where X represents the $M, N, \cdots$ higher shells, which give rise to the $L_l+L\alpha_{1,2}+L\beta_{2,15}$ components of the L x-ray spectrum at $Z=64$ and 67. The factor $C_{(K\alpha_1)}$ is the number of coincident $K\alpha_1$ x-ray counts in the $K\alpha_1$ gate $G1$, corrected for background. (The use of parentheses is to indicate a *coincidence* intensity, to distinguish the *singles* intensity $I_{K\alpha_1}$ in the spectrum defined by gate $G1$.)

The factor $C_{L_3X(K\alpha_1)}(\theta)$ is the total number of L x-ray counts, gated by $K\alpha_1$ x rays arising from L_3-X transitions and corrected for background, nuclear cascading if present, chance coincidences, and for the directional correlation[9] in the 180° coincidence geometry used. $C_{(K\alpha_2)}$ is the number of coincident $K\alpha_2$ counts in gate $G2$, corrected for background and for the number of coincident $K\alpha_1$ tail events falling in gate $G2$. $C_{L(K\alpha_1)}(\theta)$ is the total number of L x-ray counts gated by $K\alpha_1$ x rays, corrected for background, nuclear cascading if present, chance events, and directional correlation.[9]

The correction for nuclear cascading and chance coincidences follows the method developed by McGeorge *et al.*[11] and is based on the fact that detection of $K\beta$ x rays indicates K-shell vacancies which have been shifted to shells higher than the L shell, the only sources of L x rays in coincidence with a $K\beta$ x-ray gate then being nuclear cascading if present and chance events. Unfortunately, in Ref. 11 an error in the equations led to an erroneous result for f_{23} at $Z=65$, although the principle of the method was correct. The L x-ray coincidence spectra corrected properly for nuclear cascading and chance events are the differences

$$C_{L(G1)}-C_{L(K\beta)}\,(I_{K\alpha_1}/I_{K\beta})$$

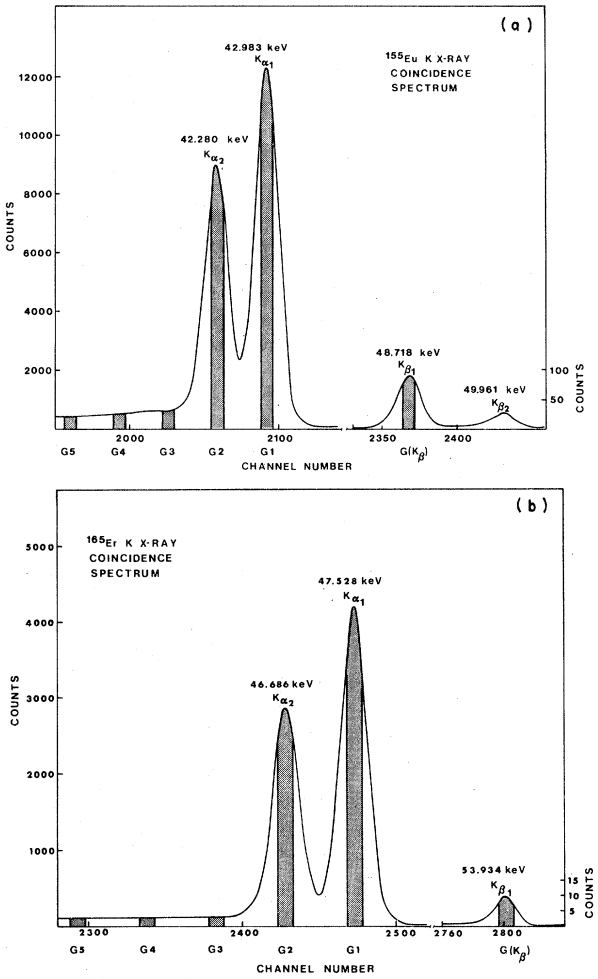

FIG. 1. (a) K x rays from 4.68-y ^{155}Eu in coincidence with L x rays. (b) K x rays from 10.4-h ^{165}Er in coincidence with L x rays. The coincidence gates $G1$, $G2$, $G3$, $G4$, $G5$, and $G(K\beta)$, indicated by the shaded areas, are set in the process of data analysis, since the three-parameter XX'-t system stores all coincidences event by event on magnetic tape.

and

$$C_{L(G2)} - C_{L(K\beta)}(I_{K\alpha_2}/I_{K\beta}),$$

where $C_{L(G1)}$ and $C_{L(G2)}$ are the gross L x-ray coincidence spectra, corrected for background, gated by $K\alpha_1$ and $K\alpha_2$ gates $G1$ and $G2$, respectively, and $I_{K\beta}$, $I_{K\alpha_1}$, and $I_{K\alpha_2}$ are the respective *singles* intensities, corrected for background, in gates $G(K_\beta)$, $G1$, and $G2$, respectively, as shown in Fig. 1. The ratios $(I_{K\alpha_1}/I_{K\beta})$ and $(I_{K\alpha_2}/I_{K\beta})$ are normalization factors needed to correct for the difference in the emission probabilities of $K\alpha_1$ and $K\beta$ and of $K\alpha_2$ and $K\beta$ x rays. These ratios are determined in the experiment and agree well with the theoretical values of Scofield.[12]

As indicated above, it is necessary to determine and correct for the number of $K\alpha_1$ tail events falling in the $K\alpha_2$ peak gate $G2$ in coincidence with the L x-ray spectrum. In all previous work reported in the literature, this correction has been made by normalizing a singles γ-ray line shape to the $K\alpha_1$ peak and then subtracting its tail from the $K\alpha_2$ peak. In the lower regions of Z where the $K\alpha_1$ and $K\alpha_2$ x rays exhibit appreciable overlap due to inadequate resolution, this procedure has been shown by us to overcorrect for the tailing,[8] because the tail from a singles peak is somewhat higher than that from a coincidence peak.

The working equation for determining the number of $K\alpha_1$ tail events in the $K\alpha_2$ gate in coincidence with L x rays, as applied in the present determination, is given by

$$N_2(2) = N_2 - N_3\left[\frac{N_1}{N_2(2)}\right] + N_4\left[\frac{N_1}{N_2(2)}\right]^2 - N_5\left[\frac{N_1}{N_2(2)}\right]^3\left[\frac{N_2(2)}{N_1+N_2(2)}\right], \quad (5)$$

where N_1, N_2, N_3, N_4, and N_5 are the total numbers of $K\alpha_{(1+2)}$ events in gates $G1$, $G2$, $G3$, $G4$, and $G5$ shown in Fig. 1, respectively, and set in accordance with the exact procedure developed in Ref. 8. The quantity $N_2(2)$ is the net number of coincident $K\alpha_2$ events, after correction for $K\alpha_1$ tailing, in gate $G2$, which is the one set at the $K\alpha_2$ peak; i.e., $N_2(2) = N_2 - N_2(1)$, where $N_2(1)$ is the number of coincident $K\alpha_1$ tail events falling in the $K\alpha_2$ coincidence gate $G2$ and is the sum of the second, third, and fourth terms in Eq. (5).

Having thus determined the net number of pure $K\alpha_2$ coincident events in the $K\alpha_2$ gate $G2$, $N_2(2)$, the coincident L x-ray spectrum is then corrected for the presence of $L_l + L\alpha_{1,2} + L\beta_{2,15}$ x-ray components arising from coincidences with $K\alpha_1$ tail events in the $K\alpha_2$ gate. The remaining $L_l + L\alpha_{1,2} + L\beta_{2,15}$ x rays then must arise from L_3 subshell vacancies produced only from Coster-Kronig transitions shifting L_1 and L_2 vacancies into the L_3 subshell. These remaining $L_l + L\alpha_{1,2} + L\beta_{2,15}$ x rays are the difference

$$C_{L_3X(G2)} - N_2(1)\left[\frac{C_{L_3X(K\alpha_1)}(\theta)}{N_1}\right].$$

Quantities that involve the L_3-K transition must also be corrected for directional correlation effects, whereas the L_2-K transition is isotropic.[9] For our 180° coincidence geometry, the corrected value of the number of L x-ray counts, gated by $K\alpha_1$ x rays, arising from L_3-X transitions is

$$C_{L_3X(K\alpha_1)}(\theta) = \frac{C_{L_3X(K\alpha_1)}}{(1+\bar{A}_{22}f_\Omega)}, \quad (6)$$

where $C_{L_3X(K\alpha_1)}$ is the experimental value uncorrected for directional correlation. $\bar{A}_{22}$ is the average directional coefficient,[9] the numerical value of which is given theoretically by Scofield,[13] and f_Ω is the finite solid angle[9] given by

$$f_\Omega = \tfrac{1}{2}\cos\theta_m(1+\cos\theta_m), \quad (7)$$

where θ_m is the half angle subtended by the detector.

The final correction to be made arises from the unresolved $L\eta$ x ray, which falls in the $L\alpha$ x-ray peak, for which the method of McGeorge *et al.*[14] is applied. On the assumption that the detection efficiencies $\epsilon_{L\alpha} \approx \epsilon_{L\eta}$, the correct value of f_{23} may be calculated from the formula

$$f_{23} = f'_{23} - \left[\frac{(L\eta/L_2)(\omega_2/\omega_3)}{(L\alpha/L_3)}\right]k, \quad (8)$$

where f'_{23} is the uncorrected value, $(L\eta/L_2)$ is the intensity ratio of the $L\eta$ component to all x rays emitted in transitions to the L_2 subshell, $(L\alpha/L_3)$ is the intensity ratio of the $L\alpha$ component to all x-rays emitted in transitions to the L_3 subshell, and k is the fraction of $L\eta$ x rays included in the $L\alpha$ x-ray peak. The value of k depends on the detector resolution, the energy separation between the $L\eta$ and the $L\alpha$ x-ray peaks (increasing with Z), and the method used to evaluate the $L\alpha$ x-ray intensity. For $Z \leq 70$, with modern Si(Li) L x-ray detectors, the value $k \approx 1$. The theoretical values of Scofield[15] are used for the ratios $(L\eta/L_2)$ and $(L\alpha/L_3)$ and are in good agreement with experiment.

Two additional very small corrections to be considered are (1) subtraction of the continuum under the peaks and (2) subtraction of $L\beta$ and $L\gamma$ tail events from the $L\alpha$ x-ray peak. (In the present work these corrections are negligible, e.g., $\leq 0.4\%$ and $\leq 0.1\%$, respectively, for both nuclides.)

III. EXPERIMENTAL

The radioactive sources used were carrier-free 4.68 y ^{155}Eu and high specific activity 10.4 h ^{165}Er. The latter was prepared by irradiating 2 mg of 67% enriched $^{164}Er_2O_3$ for 4 h at 10^{13} n/cm^2 sec in the Georgia Tech Research Reactor. The irradiated sample was then dissolved in 1 ml of hot 3M HNO_3, and 5 to 10 μl aliquots were drop evaporated onto 0.25 mm thick Mylar discs, which were then lightly sealed with Krylon spray. The radioactive side was positioned to face the L x-ray detector in order to minimize attentuation of L x rays. While counting the ^{155}Eu source, a 100 mg/cm^2 plastic absorber was placed between the source and the K x-ray detector to remove most of the beta particles, to reduce the β^- continuum. This was unnecessary for ^{165}Er, which decays purely by electron capture to the ground state of ^{165}Ho.

The electronic block diagram is shown in Fig. 2. The dashed portion is used to acquire simultaneous singles spectra for measurements of ω_2 and ω_3, and the solid lines in the diagram represent the three-parameter coincidence experiment for determination of f_{23}. The logic gate width typically is 2 μsec, and the system resolving time is 50 to 70 nsec (full width at half amplitude). The multiparameter analyzer is a computer-based Nuclear Data ND-4420 system that requires all input signals to arrive within an interval of 2 μsec in order to be stored as coincidences, which is done event by event on magnetic tape. By using an

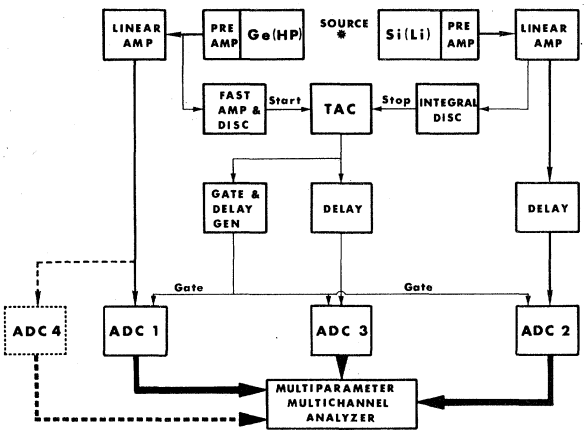

FIG. 2. The electronic block diagram for the three-parameter $XX \cdot t$ coincidence system. The heavy lines indicate the path of the digital signals, the medium lines represent analog signals, and the fine lines carry the logic pulses. The dashed portion is used to acquire simultaneous singles spectra for measurement of ω_2 and ω_3. The parameters of the system are described in the text.

$XX \cdot t$ three-parameter arrangement, a broad TAC spectrum of approximately 500 nsec can be acquired, and then a narrow, prompt portion of the TAC spectrum can be selected in the data analysis. The ratio of the counts in the narrow, prompt TAC gate to those in the broad TAC spectrum is used to determine the coincidence efficiency, which is typically in the range of 60 to 65% for the narrow TAC gate, assuming the coincidence efficiency to be unity for the broad TAC spectrum.

A very narrow TAC window (50–70 nsec FWHA), was used, in spite of the fact that this produced a coincidence efficiency of only 60 to 65%. This sacrifice of some coincidence efficiency was made in order to achieve a significant reduction in tailing in the K and L x-ray spectra, where rejection of slow pulses is achieved by using the very narrow TAC window.[8]

The K x-ray detector is a ruggedized ion-implanted planar ORTEC Ge(HP) (which exhibits a resolution under the coincidence conditions described above of 340 eV FWHM at 46 keV and a peak/tail ratio of 70:1) and the L x-ray detector is a planar Kevex Si(Li) (coincidence resolution of 240-eV FWHM at 5.9 keV), using a 1.5-μsec amplifier time constant for each detector. Both detectors are fitted with 5-ml (0.125-mm) Be windows and were used in 180° coincidence geometry. In the experimental setup, collimation was employed to reduce drastically the Compton backscattering. This especially benefitted the L x-ray spectrum, almost completely removing the Compton continuum. The graded collimator consisted of 1.8-mm Pb, 0.6-mm Cd, 0.9-mm Cu, and 1-mm Al, placed back to back on each side of the radioactive source. The center hole was approximately 5.5 mm in diameter. An example of the K spectrum is shown in Fig. 1 and the L spectra in Figs. 3 and 4.

In order to determine ω_2 and ω_3, it is necessary to establish the detection efficiency of the L x-ray detector. This was done by using calibration standards of ^{57}Co, from the Laboratoire de Métrologie des Rayonnements Ionisants, Gif-sur-Yvette, France, and ^{54}Mn from the Physikalisch-Technische Bundesanstalt, Braunschweig, West Germany. Campbell *et al.*[16] have demonstrated that the use of drop-evaporated radioactive sources as standards, calibrated as γ-ray standards, can result in the determination of efficiency points in the 5- to 40-keV region that may be as much as 3 to 16% too low, owing to self-absorption and the use of X/γ ray intensity ratios, the self-absorption being negligible for the much higher energy γ ray for which the calibration was done. Another major source of error in the efficiency calibration is the presence of small variations in

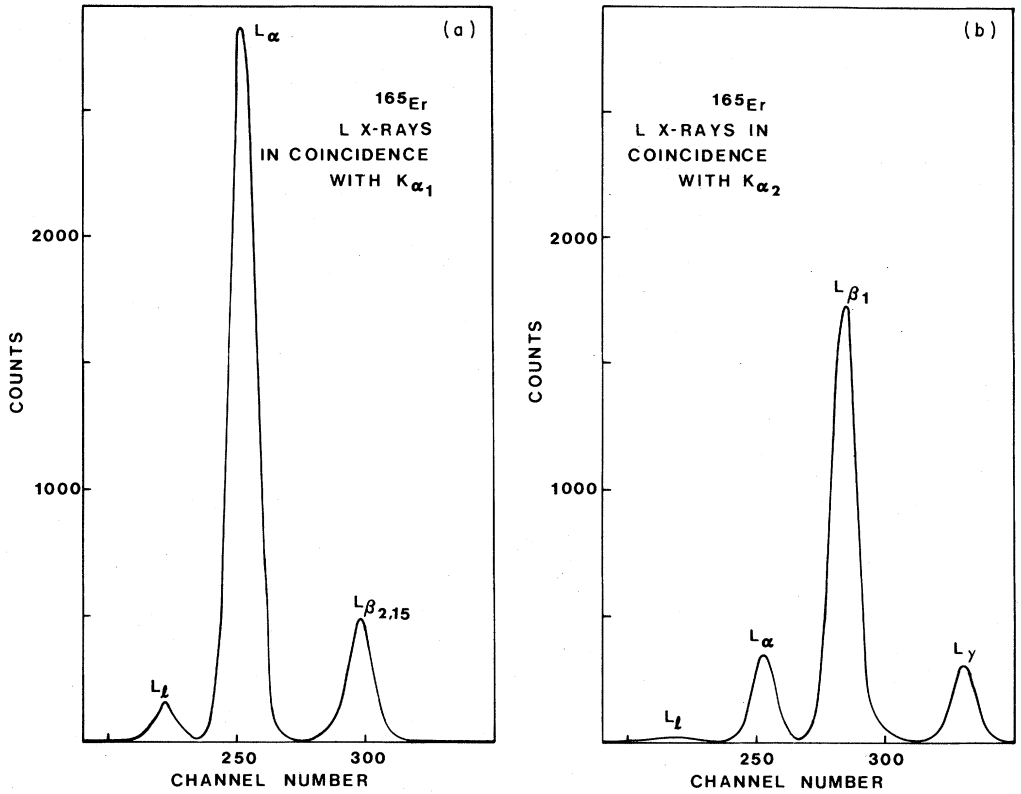

FIG. 3. (a) The L x-ray spectrum gated by $K\alpha_1$ x rays at $Z=64$ from decay of 4.68-y ^{155}Eu. (b) Similar L x-ray spectrum, but gated by $K\alpha_2$ x rays.

source position, not only in distance from the detector, but also in lateral deviation from the axial center.[17] A 5% variation in a 2-cm source-to-detector distance for a 20-mm diameter × 3-mm thick detector can cause a shift in the efficiency by as much as 8%.[18] It is due to possible systematic errors of this magnitude that inherent errors of up to 11% in the efficiency calibration of the L x-ray detector may be present, and it is this uncertainty that is the major contribution to the un-

TABLE I. Corrections applied to the K x-ray gates and the gated L x-ray spectra.[a]

	^{155}Eu				^{165}Er			
Component	$G1$ (%)	$G2$ (%)	$L_{(K\alpha_1)}$ (%)	$L_{(K\alpha_2)}$ (%)	$G1$ (%)	$G2$ (%)	$L_{(K\alpha_1)}$ (%)	$L_{(K\alpha_2)}$ (%)
Continuum	0.3	0.4			≤0.1	0.18		
Chance coincidences and nuclear cascades			17.9	13.8			0.5	0.4
Tailing of $K\alpha_1$ events into the $K\alpha_2$ gate		5.0				3.8		
Directional correlations			2.5				2.5	
$\ell\ell + L\alpha_{1,2} + L\beta_{2,15}$ (i.e., L_3X) counts in gate $G2$ caused by $K\alpha_1$ tail events				23.0				21.7
Tailing of $L\beta + L\gamma$ events into the $L\alpha$ peak			≤1.0	2.0			≈0	≈0
Percentage of net true coincidence events	99.7	94.6	≥78.6	61.2	≥99.9	96.0	97.0	77.7

[a] $G1$ is the $K\alpha_1$ gate and $G2$ is the $K\alpha_2$ gate; $L_{(K\alpha_1)}$ and $L_{(K\alpha_2)}$ are the total L x-ray spectra produced by gates $G1$ and $G2$, respectively.

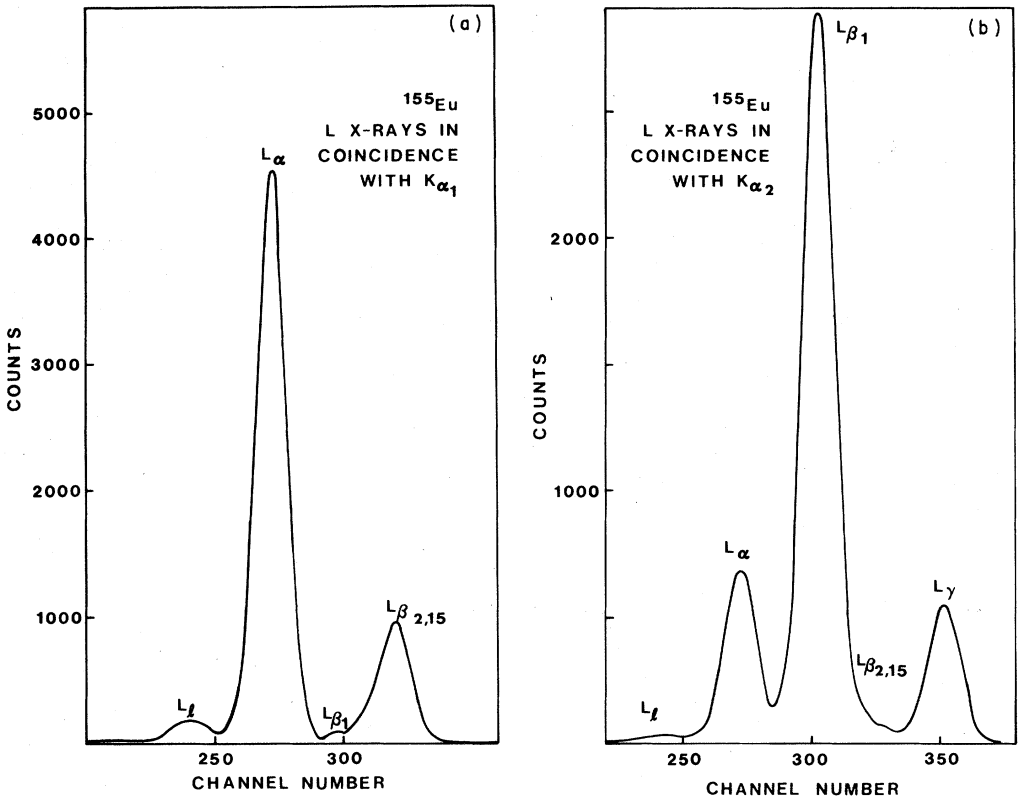

FIG. 4. (a) The L x-ray spectrum gated by $K\alpha_1$ x-rays at $Z=67$ from decay of 10.4-h ^{165}Er. (b) Similar L x-ray spectrum, but gated by $K\alpha_2$ x rays.

certainty limits placed on the determination of ω_2 and ω_3 in the present work. Since the detection efficiencies are not involved in the determination of f_{23}, these systematic errors are absent in the measurement of f_{23}.

The coincidence experiment to determine f_{23} was repeated for each nuclide four times, the last two of which included the measurements of ν_2 and ω_3. Each run required approximately one week of counting time in order to reduce the statistical errors in counting to less than 1% in the coincidence gates and coincidence spectra.

IV. RESULTS AND ANALYSIS OF ERRORS

The data were evaluated according to the procedure given in Sec. II and the various contribu-

TABLE II. Quantities used to evaluate ν_2, f_{23}, and ω_3.

	$Z=64$			
Quantity [a]	Value	% error	Value	% error
$C_{L(K\alpha_2)}$	78 000	0.4%	54 850	0.4%
$I_{K\alpha_2}$	8.91×10^{7}	0.1%	5.05×10^{7}	0.1%
ϵ_L	7.52×10^{-3}	11%	8.75×10^{-3}	11%
ϵ_c	0.6276	0.15%	0.6059	0.15%
$C_{L_3X(K\alpha_2)}$	9 037	2.5%	3 475	2.7%
$C_{(K\alpha_1)}$	104 150	0.3%	42 350	0.5%
$C_{L_3X(K\alpha_1)(\theta)}$	78 860	1.0%	39 990	1.0%
$C_{(K\alpha_2)}$	71 770	2.4%	27 925	2.6%
$C_{L(K\alpha_1)(\theta)}$	122 900	1.0%	86 510	1.1%
$L_{K\alpha_1}$	1.62×10^{8}	0.08%	9.06×10^{7}	0.1%

[a] See Eqs. (1)–(3) in the text. These values represent results and error limits from a typical run on each nuclide.

tions to the coincidence gates and coincidence L x-ray spectra are listed in Table I in the order in which the corrections are applied. The quantities needed for determining ν_2, f_{23}, and ω_3 from Eqs. 1, 2, and 3 are listed in Table II, with numerical results and percent errors for a typical run for each nuclide. Details of the error evaluations are given below.

In order to establish the independence of the values determined for ν_2, f_{23}, and ω_3 with respect to the location of the K x-ray gates $G1$ and $G2$, in each run $G1$ and $G2$ were analyzed for positions immediately below, at, and above the peak centroids. The resulting values exhibited a random distribution about the mean, thus assuring the validity of the tailing correction for $K\alpha_1$ events in gate $G2$. However, tailing in the coincident L x-ray spectra was at a minimum when gates $G1$ and $G2$ were chosen at the centroids of the K x-ray peaks. The percent errors listed in Table II from a typical run on each nuclide are purely statistical, except for ϵ_L, $C_{L_3X(K\alpha_2)}$, and $C_{(K\alpha_2)}$ which are dominated by the presence of systematic uncertainty.

From the four runs, a total of 12 values of f_{23} was obtained, and their mean value is listed in Table III with an uncertainty of twice the average deviation from the mean, arising primarily from systematic error. All previous determinations of f_{23} contained estimated systematic errors that are two to three times larger than those in the present work. The uncertainty limits on ω_2 and ω_3 values are completely dominated by the systematic error arising in the L x-ray detection efficiency ϵ_L (see Table II).

Previous measurements[5,6] of the L-subshell fluorescence yields, ω_2 and ω_3, are in approximate agreement with the present results within the error limits. However, the previous values[5,7] of f_{23} lie significantly above the present ones and are outside experimental error limits. High values can result from the following experimental difficulties[5,7]: lack of sufficient energy resolution in the K and L x-ray detectors required to reduce the tailing correction to a minimum, use of a singles γ-ray line shape to estimate the tailing of $K\alpha_1$ events in the $K\alpha_2$ peak, apparent lack of correction for $L\beta$ tailing into the $L\alpha$ peak, lack of sufficiently narrow prompt time gating in the two-parameter coincidence technique used,[5,7] and lack of collimation to reduce the Compton continuum from backscattered events.

TABLE III. Final values of ν_2, f_{23}, ω_3 and ω_2 from the present work.

Quantity	$Z=64$	$Z=67$
ν_2	0.184 ± 0.022	0.204 ± 0.023
f_{23}	0.130 ± 0.012	0.115 ± 0.011
ω_3	0.161 ± 0.019	0.180 ± 0.020
ω_2	0.165 ± 0.022	0.186 ± 0.023

V. DISCUSSION

The nonrelativistic theoretical calculation of McGuire[2] at $Z=67$ predicts $\omega_2=0.203$, $\omega_3=0.201$, and $f_{23}=0.138$, all of which lie considerably above the present experimental values. Chen and Crasemann[3] predict from a nonrelativistic independent-particle model values at $Z=67$ of $\omega_2=0.190$ and $f_{23}=0.147$. Although the predicted value of ω_2 agrees well with the present experiment, the value of f_{23} is much too large, as has been found by Nix and Fink[19] in a systematic comparison of theory and experiment for f_{23} vs Z. The 1971 nonrelativistic calculations of Chen, Crasemann, and Kostroun[4] also predict values of f_{23} which exceed the trend of experimental results, although the theoretical predictions of ω_2 and ω_3 agree with the present results.

The 1979 relativistic calculations of Chen *et al.*,[1] do not extend below $Z=70$. However, a linear extrapolation to $Z=64$ indicates good agreement with the present experimental values of ω_2. Extrapolation to $Z\leq 70$ for f_{23} is not feasible, but it would appear to result in values much larger than the present experimental ones. We are extending the present measurement technique to $Z=54$ and to $Z=82$ to provide a more general critical test of theory.

The origin of the rather serious disagreement between theory and experiment for f_{23} can no longer be ascribed to error in the experiments, nor can it arise from the small admixture of double vacancies from K-LL and K-LM Auger transitions, since this effect has been shown at $Z=49$,[20] 73,[21] and 82 (Ref. 22) to be less than about 10% on L-fluorescence yields and is probably altogether negligible for f_{23}.

ACKNOWLEDGMENTS

We thank Mr. R. C. McFarland and Mr. R. S. Kirkland of the Georgia Tech Research Reactor for irradiations.

[1]M. H. Chen, E. Laiman, B. Crasemann, M. Aoyagi, and Hans Mark, Phys. Rev. A 19, 2053 (1979); Bull. Am. Phys. Soc. 24, 624 (1979).
[2]E. J. McGuire, Phys. Rev. A 3, 587 (1971).
[3]M. H. Chen and B. Crasemann, in *Inner Shell Ionization Phenomena and Future Applications*, edited by R. W. Fink, S. T. Manson, J. M. Palms, and P. V. Rao (U.S. Atomic Energy Commission, 1973), p. 43.
[4]M. H. Chen, B. Crasemann, and V. O. Kostroun, Phys. Rev. A 4, 1 (1971).
[5]D. G. Douglas, Can. J. Phys. 50, 1697 (1972).
[6]C. P. Holmes and V. O. Kostroun, Bull. Am. Phys. Soc. 15, 561 (1970).
[7]D. G. Douglas, Can. J. Phys. 54, 1124 (1976).
[8]B. E. Gnade, R. A. Braga, W. R. Western, J. L. Wood, and R. W. Fink, Nucl. Instrum. Methods 164, 163 (1979).
[9]W. Bambynek, B. Crasemann, R. W. Fink, H. U. Freund, Hans Mark, C. D. Swift, R. E. Price, and P. V. Rao, Rev. Mod. Phys. 44, 716 (1972).
[10]P. V. Rao, R. E. Wood, J. M. Palms, and R. W. Fink, Phys. Rev. 178, 1997 (1969).
[11]J. C. McGeorge, H. U. Freund, and R. W. Fink, Nucl. Phys. A154, 526 (1970).
[12]J. H. Scofield, At. Data Nucl. Data Tables 14, 121 (1974).
[13]J. H. Scofield, Lawrence Livermore Laboratory Report UCRL-51231, 1972 (unpublished).
[14]J. C. McGeorge, S. Mohan, and R. W. Fink, Phys. Rev. A 4, 1317 (1971).
[15]J. H. Scofield, Phys. Rev. 179, 9 (1969).
[16]J. L. Campbell, H. H. Jorch, and J. A. Thompson, Nucl. Instrum. Methods 140, 167 (1977); 143, 551 (1977).
[17]Z. B. Alfassi and R. Nothman, Nucl. Instrum. Methods 143, 57 (1977).
[18]G. Bertolini and G. Restelli, in *Atomic Inner-Shell Processes*, edited by B. Crasemann (Academic, New York, 1975), Vol. 2, p. 123.
[19]D. W. Nix and R. W. Fink, Z. Phys. A273, 305 (1975).
[20]P. A. Indira, I. J. Unus, P. V. Rao, and R. W. Fink, J. Phys. Atom. Molec. Phys. (London) B12, 1351 (1979).
[21]J. L. Campbell, L. A. McNelles, J. S. Geiger, J. S. Merritt, and R. L. Graham, Can. J. Phys. 55, 868 (1977).
[22]P. V. Rao, R. E. Wood, and V. R. Veluri, J. Phys. Atom. Molec. Phys. (London) B10, 399 (1977).